第 48 卷 第 11 期/2021 年 6 月/中国激光 研究论文

中国激光

基于液晶空间光调制器进行光谱调制的飞秒啁啾脉冲放大系统

段雨飞[1,2]，李峰[1*]，杨直[1]，李强龙[1]，杨洋[1]，吴天昊[1,2]，王屹山[1]，杨小君[1**]

[1]中国科学院西安光学精密机械研究所瞬态光学与光子技术国家重点实验室，陕西 西安 710119；

[2]中国科学院大学，北京 100049

摘要 飞秒光纤激光器具有良好的光束质量与稳定性，被广泛应用于精细材料加工行业。目前工业化光纤飞秒激光器主要是通过啁啾脉冲放大系统的多级放大来实现其高功率，可是多级放大过程会导致严重的增益窄化效应，限制最终的压缩脉冲宽度。为了解决增益窄化问题，缩短脉冲宽度，提高峰值功率，达到更好的“冷”加工效果，提出一种基于空间光调制器的光谱整形系统，通过加载到空间光调制器上的灰度图，产生中心凹陷、平顶等特殊光谱形状，放大后的光谱宽度与初始的种子源保持一致。与未加光谱调制相比，光谱调制后的光谱宽度从 7 nm 提高到 9.5 nm，对应的极限脉宽从 222 fs 减少到 164 fs 左右。最后通过透射式光栅对压缩，得到了平均功率为 1.3 W 的飞秒激光输出，采用高斯拟合的方式测量脉冲，脉冲宽度为 170 fs，接近转换极限脉冲。

关键词 激光器；液晶空间光调制器；光纤飞秒激光器；光谱调制；增益窄化；啁啾脉冲放大系统

中图分类号 TN248 **文献标志码** A **doi**：10.3788/CJL202148.1101001

1 引 言

超短脉冲激光器特别是飞秒激光器在阿秒光源、光镊、精细加工、玻璃焊接和双光子聚合等方面得到了广泛应用[1-5]。目前，工业用大功率飞秒激光器主要包括碟片激光器[6]、板条激光器[7]与光纤激光器[8]。与其他激光器相比，光纤激光器具有结构紧凑、光束质量好、系统稳定和散热性好等优点，被广泛应用于各种激光应用领域，特别是精细材料加工领域[9]。但是，目前飞秒光纤激光器主要是通过啁啾脉冲放大技术(CPA)来降低放大过程中的非线性与器件损伤，最后获得高功率、窄脉宽的飞秒激光以满足激光加工领域的要求[10]。随着工业化光纤飞秒激光器的发展以及所需能量的提升，整个激光系统势必朝着多级放大的方向发展。随着放大级次的增加，放大系统中增益介质增益不均匀造成的增益窄化效应就会愈加明显，光谱窄化严重，从而压缩后的极限脉冲宽度增大，脉冲峰值功率降低，严重影响加工效果以及加工过程中的热扩散。为了达到符合要求的峰值功率，不仅需要提升输出的脉冲能量，还需要有效控制最终输出的脉冲宽度。而光纤放大受到非线性效应的限制，能量的提升一直是一大瓶颈问题。在同等输出能量条件下，消除放大过程中的增益窄化效应，保证最终的压缩脉宽是提高峰值功率的重要途径。

目前，解决光纤激光器增益窄化问题的途径有自相位调制[11]、新型放大级系统[12]、偏振光调制[13]和介质层滤波器[14]等。但上述方法只能实现固定的光谱调制，难以解决不同放大系统或者同一放大系统不同功率要求下的增益窄化问题。因此，人们提出利用可编程元件来实现光谱调制的可控性。其中，液晶空间光调制器((LC-SLM))作为光束整形与脉冲整形的常用元件[15]，与一般声光滤波器[16]相比，调节精度更高。对于光纤激光器的种子源来说，其光谱宽度只有几纳米或者十几纳米[17]，显然液晶空间光调制器更适合于调制光纤激光器的光

收稿日期：2020-10-26；**修回日期**：2020-12-05；**录用日期**：2020-12-23

基金项目：国防基础科研计划(JCKY2016130B203)、国家自然科学基金(61690222，61805274)

*E-mail：lifeng@opt.ac.cn；**E-mail：yxj@opt.ac.cn

谱。2014 年，安国等[18]利用电寻址的反射式空间光调制器对光纤频率梳信号源进行整形，最后得到了平坦型、三角形等频谱形状。本文基于空间光调制器的特性以及啁啾脉冲放大系统对光谱调制的需要，提出了基于二维强度型液晶空间光调制器进行光谱调制的光谱整形系统方案，并搭建了啁啾脉冲放大系统，实现了消除增益窄化的目的，获得了更窄的脉冲宽度输出。

2　实验装置与原理

2.1　实验装置及步骤

该系统主要包括四个组成部分：全光纤种子源以及单模预放大系统、以空间光调制器为主要器件的整形系统、全光纤主放大系统和光栅对压缩系统。实验装置如图 1 所示。其中，使用的种子源是基于可饱和吸收镜（SESAM）锁模技术的全光纤超短脉冲振荡器，最大输出功率为 10 mW，光谱宽度为 7.5 nm，重复频率为 40 MHz，脉冲宽度为 10 ps，中心波长为 1031 nm。考虑到整体光谱整形系统的损耗较大问题，在种子源后加入一级单模光纤预放大器，其中泵浦光源为中心波长为 976 nm、最大功率为 400 mW 的光纤耦合半导体（LD），增益光纤为 0.6 m 长的保偏单模掺镱光纤（Nufern PM-YSF-H1-HP），纤芯直径为 4 μm，通过预放大器后的信号光经熔接在光纤上的小型透镜准直后进入到光谱整形系统中，并测得进入光谱整形系统的光功率为 55 mW。整形系统包括一个半波片、一个偏振分光棱镜（PBS）、光栅、准直透镜和液晶空间光调制器。半波片与分光棱镜的作用是改变信号光的偏振方向，使其与空间光调制器的液晶屏长边平行，利用 1450 line/mm 的光栅将光谱分开，分开后的长条形发散光谱通过透镜准直，并且最后进入反射式液晶空间光调制器进行各个波长的强度调制，调制后的光谱再一次按原光路返回后，水平方向的偏振光通过 PBS 后经反射镜组耦合进入主放大系统中。主放大系统是由两级放大系统组成，其中第一级放大是由纤芯直径为 10 μm 且包层直径为 125 μm 的双包层掺镱保偏光纤、隔离器、泵浦源等相关器件组成；另一级放大是由 2 m 长的纤芯直径为 25 μm、包层直径为 250 μm 的大模场掺镱增益光纤、泵浦源组成。另外，在光纤输出端斜切一个 8°角以防止反馈光和后向放大，保护放大系统。主放大部分仍采用 9 W LD 进行泵浦，可得到 2 W 的输出光。光栅对压缩系统是由一块焦距为 12.5 mm 的非球面准直透镜、两块 45°高反镜、两块 1450 line/mm 光栅和一块屋脊棱镜组成。放大后的激光首先经过非球面透镜进行准直，然后经过第一块反射镜，再以利特罗角进入光栅对中，在 1450 line/mm 光栅对中压缩后，被第二个高反镜导入自相关仪中，最后通过自相关仪对输出激光的脉宽进行测量。

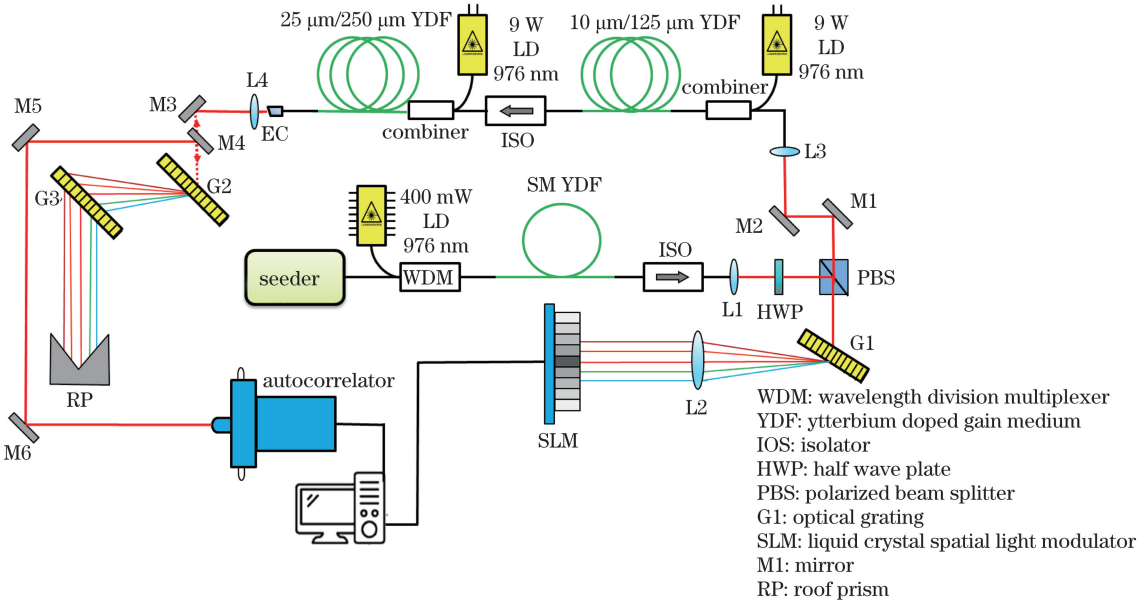

图 1　整形压缩系统的实验装置图

Fig. 1　Experimental setup of shaping-compression system

2.2　液晶空间光调制器

液晶空间光调制器根据控制信号的不同分为光寻址与电寻址两种调制类型，其中电寻址空间光调制器具有功耗低、体积小、抗干扰能力强、响应速度

快等[19]优点，受到广泛关注。电寻址空间光调制器就是通过电压来控制液晶的扭曲方向，进而通过改变其折射率与偏振方向，实现相位与振幅调制，具体原理如图 2 所示。

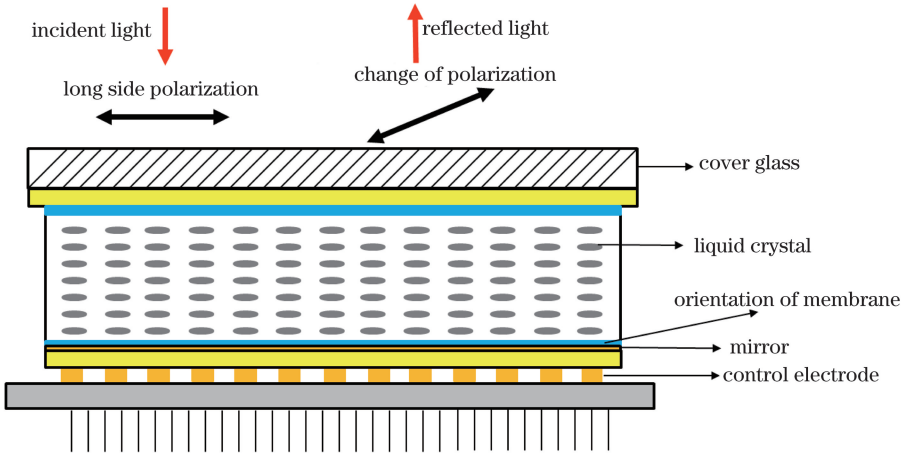

图 2　反射式液晶空间光调制器的原理图

Fig. 2　Principle diagram of reflective liquid crystal spatial light modulator

液晶分子位于屏幕的前后表面之间，面向分子的屏幕面经过预处理，液晶分子顺着屏幕面上的沟槽整齐排列。加上电压之后，液晶发生一定的偏转，偏振方向不再与液晶调制器的长边方向平行，从而达到振幅调制的效果。同时，由于液晶排列方式的改变，其折射率发生变化，进而实现相位调制。根据输出光的不同，液晶空间光调制器可以分为反射式与透射式两种，考虑到整形系统的效率以及光路的复杂性，本实验选用的是反射式的振幅型液晶空间光调制器，型号为 FSLM-HD70-A/P，其具体参数如表 1 所示。

表 1　空间光调制器参数

Table 1　Parameters of spatial light modulator

Parameter	Content	Parameter	Content
Modulation type	Amplitude modulation and phase modulation	Filling factor	87%
LCD type	Reflection type	Optical efficiency	75%
Gray type	8 bit, 256 step	Damage threshold	2W /cm^2
Number of liquid crystals in LC-SLM	1920×1080	Data interface	Digital visual interface
Element diameter	8.0 μm	Spectral range	420–1100 nm
Incident angle of light and effective area	Incident angle of 0.69′ and effective area of 15.36 mm×8.64 mm	Contrast of black color and white color	>2000∶1

光栅的衍射公式为

$$\sin\theta+\sin\varphi=m\frac{\lambda}{d},\tag{1}$$

式中：θ 为激光衍射角；φ 为入射角度；d 为光栅常数；λ 为激光波长；m 为衍射级次。由于实验所用的是一级闪耀光栅，则衍射公式变为

$$\sin\theta_0+\sin\varphi=\frac{\lambda_0}{d},\tag{2}$$

式中：θ_0 为利特罗角；λ_0 为中心波长。

同时，为了达到更大的衍射效率，令入射角等于衍射角，并且波长为中心波长 λ_0，则此时的衍射角称为利特罗角 θ_0，即

$$\theta_0=\arcsin\left(\frac{\lambda_0}{2d}\right)。\tag{3}$$

由(3)式可以算出利特罗角为 48.3°，以该角度衍射到 LC-SLM 上的位置为中心位置，记为 $x_0=0$。SLM 上每个不同位置对应于不同的波长：

$$x=f\tan\left[\arcsin\left(\frac{\lambda}{d}-\frac{\lambda_0}{2d}\right)-\arcsin\left(\frac{\lambda_0}{d}\right)\right],\tag{4}$$

式中：f 为透镜焦距。由(4)式可知，x 与 λ 一一对应，因此可以通过调节不同 x 位置处的灰度来改变光谱形状。

2.3　增益窄化以及解决方法

非线性薛定谔方程(Nonlinear Schrodinger

Equation，NLF)为

$$\mathrm{i}\frac{\partial A}{\partial z_1}=\frac{\mathrm{i}}{2}g(\omega)A+\frac{\beta_2}{2}\frac{\partial^2 A}{\partial T^2}-\gamma|A|^2A,\quad(5)$$

式中：A 为光信号的振幅；z_1 为光纤中的传播距离；$g(\omega)$为与频率 ω 有关的增益函数；β_2 为二阶色散系数；γ 为非线性系数；T 为时间。本实验采用的种子源重复频率为 40 MHz，输出激光的最大单脉冲能量为 0.5 nJ，由于单脉冲能量较小，可忽略非线性效应带来的影响，只考虑群速度色散(二阶色散)与增益系数。小信号增益[20]满足

$$g(\omega)=\frac{g_0}{1+\left[\frac{2(\omega-\omega_0)}{\Delta\omega}\right]^2},\quad(6)$$

式中：ω_0 为中心频率；$\Delta\omega$ 为整个增益介质的增益谱宽；g_0 为中心频率的峰值增益系数；$\omega-\omega_0$ 为中心频率的偏移度。若为小信号增益且不考虑增益饱和，则 g_0 为一个常数，$g_0=g_{\omega_0}$。若是大功率信号，则该增益函数与时间和位置有关：

$$g_0=g_{\omega_0}\exp\left[-\frac{1}{E_s}\int_{-\infty}^{T}|A(z,T)|^2\mathrm{d}T\right],\quad(7)$$

式中：E_s 为介质的饱和能量密度；z 为增益光纤中的传输的距离。由于本系统采用输出功率为 9 W 的泵浦源，增益光纤未达到增益饱和，属于小信号增益，因此最终的 NLF 方程为

$$\mathrm{i}\frac{\partial A}{\partial z}=\frac{\frac{\mathrm{i}}{2}g_{\omega_0}}{1+\left[\frac{2(\omega-\omega_0)}{\Delta\omega}\right]^2}A+\frac{\beta_2}{2}\frac{\partial^2 A}{\partial T^2}。\quad(8)$$

利用分步傅里叶算法对(8)式进行逆运算，将 z 变为 $-z$，然后定义进入放大系统后的光谱形状，通过逆运算得到进入放大系统之前的光谱形状，将该光谱与原始光谱进行比较，就可以得到对应的灰度图。下面以平顶光谱为例，定义其光谱形状如图 3(a)所示，通过逆运算得到进入放大系统前的光谱，如图 3(b)所示，两者相比，最终加载到 SLM 的灰度图如图 3(c)所示。

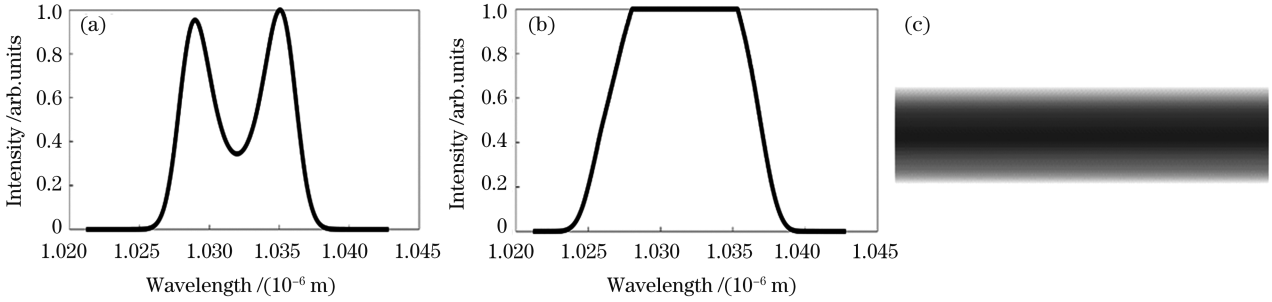

图 3　逆运算的理论模拟图。(a)定义的理想光谱形状；(b)逆运算得到的所需光谱形状；(c)所需的二维灰度图

Fig. 3　Theoretical simulation by inverse operation. (a) Defined ideal spectral shape; (b) desired spectral shape obtained by inverse operation; (c) required two-dimensional grayscale map

3　结果分析与讨论

利用以液晶空间光调制器为核心的整形系统，可以实现光谱形状的任意调节，这是本实验成功的关键。信号光经过单模预放大系统后进入到整形系统，同时通过添加灰度图将光谱整形为平顶、中心凹陷、三角形、连续凹陷等形状，对应的实际实验结果与模拟得到的灰度图如图 4 所示。由此可知，该整形系统有很好的编程性与灵活性，可以实现一定精度的光谱整形，能实现宽光谱调节。但是，由于此液晶空间光调制器的填充率只为 87%，整个液晶屏上的液晶分子间存在间隔，这些间隔不具备调节能力，从而液晶空间光调制器本身具有较为严重的调制作用，因此整形后的光谱形状不理想[15]。

为了验证其光谱增益窄化效应，分别测量进入主放大系统前的光谱宽度与经过主放大系统后的光谱宽度，结果如图 5(a)、(b)所示。可以看出，此放大系统的增益窄化效应明显，光谱宽度缩小了 1.5 nm 左右，并且由于种子源的中心波长略大于其增益介质的中心波长，中心波长略向前偏移。

最后，在二维液晶空间光调制器上加载逆运算所获得的灰度图，得到光谱整形放大后的超高斯光谱形状，如图 6 所示，可以看出，此光谱的半峰全宽为 9.5 nm 左右，展宽了 2.5 nm 左右。同时，也可以看出，实际得到的光谱形状与理论仿真得到的超高斯光谱存在差异，且中心有继续高于两侧的趋势，这说明经过更高级次的放大后，其抑制增益窄化的作用更加明显。同时，液晶空间光调制器的液晶间隔对光谱的调制作用也明显减弱，进一步说明了该系统的可行性。最终经过计算得到光栅对压缩的极

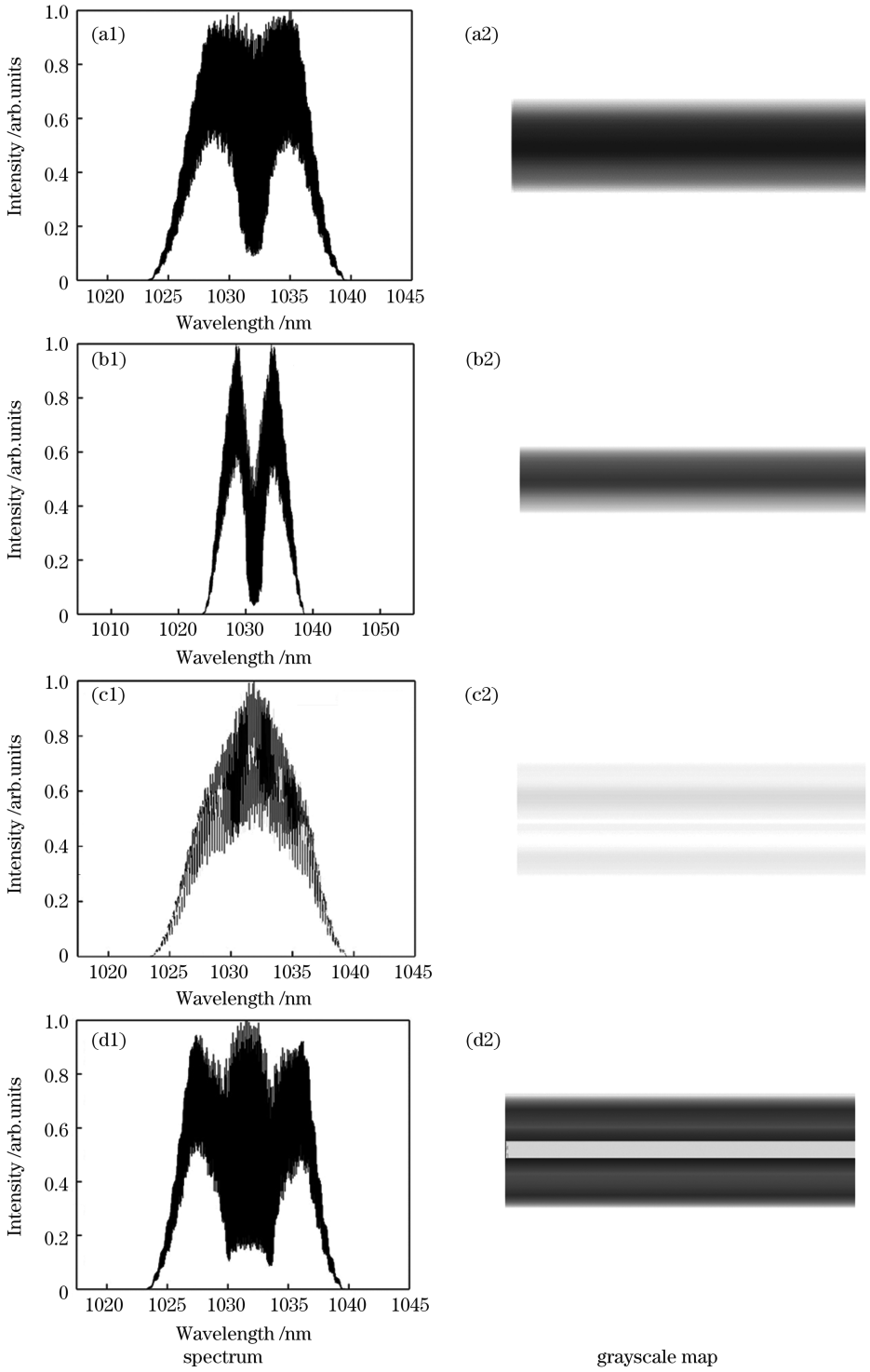

图 4 光谱整形效果及对应的灰度图。(a1)(a2)平顶型;(b1)(b2)中心凹陷型;(c1)(c2)三角形;(d1)(d2)连续凹陷型

Fig. 4 Spectral shaping effects and corresponding grayscale maps. (a1)(a2) Flat-top type; (b1)(b2) center-suppression type; (c1)(c2) triangle type; (d1)(d2) continuous suppression type

限距离为 4 cm,通过调整光栅对的间距获得理论上的最短脉宽。通过自相关仪的高斯型函数,拟合得到了光谱整形前后的对比图,如图 7(a)、(b)所示,最后得到了实际脉宽为 170 fs、平均功率为 1.3 W 的超短脉冲。由实验结果可以看出,脉宽缩短了 86 fs,其峰值功率提升了 1.5 倍。光纤激光器多级放大系统的弊端得到改善,飞秒光纤激光器更加适用于精细加工。

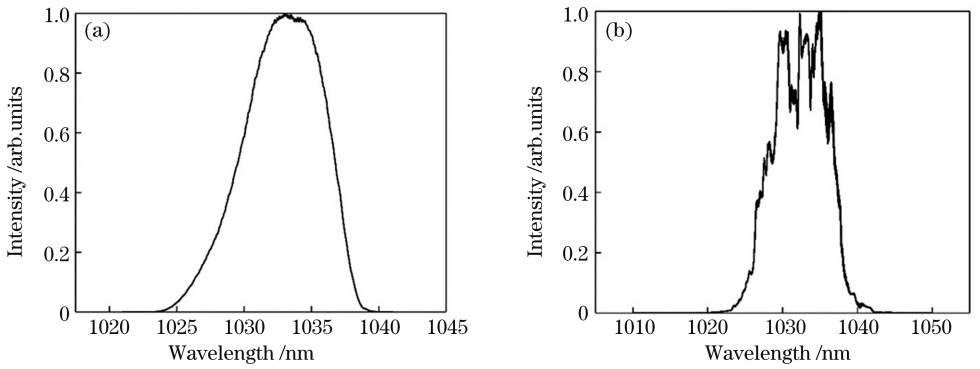

图 5 放大前后的光谱对比图。(a)进入主放大系统前;(b)经过主放大系统后

Fig. 5 Spectral comparison before and after amplification. (a) Before entering main amplification system; (b) after passing through main amplification system

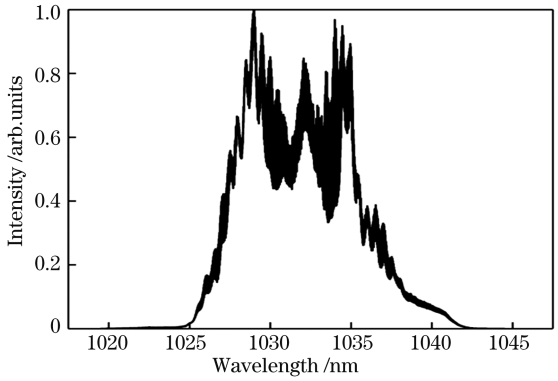

图 6 调制后的最终光谱形状

Fig. 6 Final spectral shape after modulation

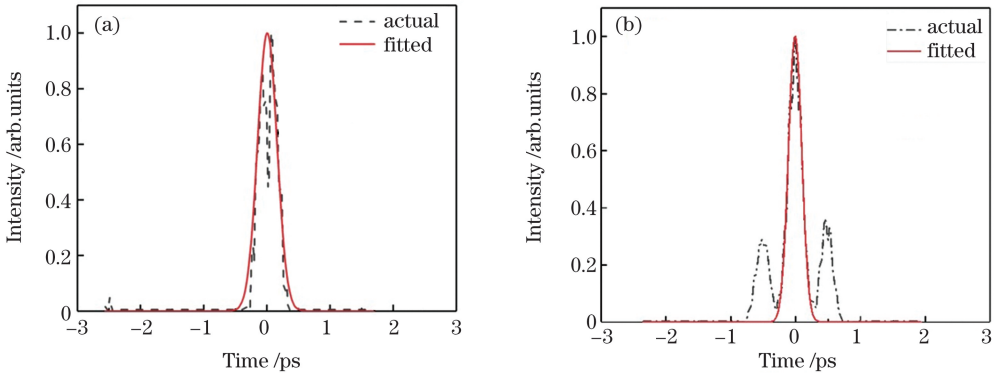

图 7 调制前后的极限脉宽对比图。(a)光谱调制前;(b)光谱调制后

Fig. 7 Limited pulse duration comparison before and after modulation. (a) Before spectral modulation; (b) after spectral modulation

4 结 论

为了抑制增益窄化效应,设计了以液晶空间光调制器为核心的光谱整形系统。该光谱整形系统通过调控不同光谱成分的增益,设置光谱带通特性,实现与后继放大光谱的动态匹配,具有调节精度高的优点,可满足不同增益条件下的光谱调制需求,得到近转化极限脉冲宽度。该系统实现了窄脉宽、高峰值功率的飞秒激光输出,达到了材料高效率冷加工的目的,可应用于对热效应要求极高的飞秒激光应用领域。下一步的工作是进行进一步的改进,增加输出功率,使用填充率更高、间隙更小的调制器进行光谱整形,以得到更好的效果。

参 考 文 献

[1] Gaumnitz T, Jain A, Pertot Y, et al. Streaking of

43-attosecond soft-X-ray pulses generated by a passively CEP-stable mid-infrared driver[J]. Optics Express, 2017, 25(22): 27506-27518.

[2] Chen Z Y, Fang G, Cao L C, et al. Direct writing of silver micro-nanostructures by femtosecond laser tweezer[J]. Chinese Journal of Lasers, 2018, 45(4): 0402006.
陈忠赟, 方淦, 曹良成, 等. 飞秒激光光镊直写银微纳结构[J]. 中国激光, 2018, 45(4): 0402006.

[3] Yuan Y J, Li X. Femtosecond laser processing of graphene and its application [J]. Laser & Optoelectronics Progress, 2020, 57(11): 111414.
原永玖, 李欣. 飞秒激光加工石墨烯材料及其应用[J]. 激光与光电子学进展, 2020, 57(11): 111414.

[4] Yu M, Huang T, Xiao R S, et al. Long focal length green femtosecond laser welding of glass[J]. Chinese Journal of Lasers, 2020, 47(9): 0902005.
于淼, 黄婷, 肖荣诗, 等. 长焦距绿光飞秒激光玻璃焊接[J]. 中国激光, 2020, 47(9): 0902005.

[5] He Z Q, Tan G J, Chanda D, et al. Novel liquid crystal photonic devices enabled by two-photon polymerization [J]. Optics Express, 2019, 27(8): 11472-11491.

[6] Russbueldt P, Mans T, Weitenberg J, et al. Compact diode-pumped 1.1 kW Yb∶YAG innoslab femtosecond amplifier[J]. Optics Letters, 2010, 35(24): 4169-4171.

[7] Tümmler J, Jung R, Stiel H, et al. High-repetition-rate chirped-pulse-amplification thin-disk laser system with joule-level pulse energy [J]. Optics Letters, 2009, 34(9): 1378-1380.

[8] Jocher C, Eidam T, Hädrich S, et al. Sub 25 fs pulses from solid-core nonlinear compression stage at 250 W of average power[J]. Optics Letters, 2012, 37(21): 4407-4409.

[9] Li F, Yang Z, Zhao W, et al. Hundred micro-joules level femtosecond fiber laser amplification system[J]. Chinese Journal of Lasers, 2015, 42(12): 1202005.
李峰, 杨直, 赵卫, 等. 百微焦级飞秒光纤激光放大系统[J]. 中国激光, 2015, 42(12): 1202005.

[10] Stark H, Buldt J, Müller M, et al. 23 mJ high-power fiber CPA system using electro-optically controlled divided-pulse amplification [J]. Optics Letters, 2019, 44(22): 5529-5532.

[11] Zaouter Y, Guichard F, Daniault L, et al. Femtosecond fiber chirped- and divided-pulse amplification system[J]. Optics Letters, 2013, 38(2): 106-108.

[12] Huynh J, Smrž M, Miura T, et al. Femtosecond Yb∶YGAG ceramic slab regenerative amplifier[J]. Optical Materials Express, 2018, 8(3): 615-621.

[13] Cao H B, Kalashnikov M, Osvay K, et al. Active spectral shaping with polarization encoding of chirped pulses in Ti∶sapphire amplifiers[C]//The European Conference on Lasers and Electro-Optics, 2017, June 25-29, 2017, Munich, Germany. Washington, DC: OSA, 2017: CA_P_17.

[14] Chiba Y H, Takada H, Torizuka K, et al. 65-fs Yb-doped fiber laser system with gain-narrowing compensation[J]. Optics Express, 2015, 23(5): 6809-6814.

[15] Wang F R, Zhang Y, Zhu Q H, et al. Theoretical study of spectral shaping by liquid crystal spatial light modulator [J]. High Power Laser and Particle Beams, 2008, 20(9): 1441-1446.
王凤蕊, 张颖, 朱启华, 等. 液晶空间光调制器光谱整形的理论研究[J]. 强激光与粒子束, 2008, 20(9): 1441-1446.

[16] Krebs N, Probst R A, Riedle E, et al. Sub-20 fs pulses shaped directly in the UV by an acousto-optic programmable dispersive filter[J]. Optics Express, 2010, 18(6): 6164-6171.

[17] Zhou J Q, Pan W W, Zhang L, et al. Research advances in mode-locked fiber lasers based on nonlinear loop mirror[J]. Chinese Journal of Lasers, 2019, 46(5): 0508013.
周佳琦, 潘伟巍, 张磊, 等. 非线性环路反射镜锁模光纤激光器的研究进展[J]. 中国激光, 2019, 46(5): 0508013.

[18] An G, Yan Q Q, Liu Y, et al. Calibration and application of optical pulse shaping system based on liquid crystal spatial light modulator [J]. Acta Photonica Sinica, 2014, 43(7): 0706012.
安国, 闫娟娟, 刘娅, 等. 基于液晶空间光调制器的脉冲整形系统校准及应用[J]. 光子学报, 2014, 43(7): 0706012.

[19] Liu Z G, Zhang T, Wang J, et al. Design and construction of the liquid crystal spatial light modulator based on the amplitude [J]. Optical Instruments, 2012, 34(3): 79-82.
刘振国, 张涛, 王健, 等. 振幅型空间光调制器的设计与实现[J]. 光学仪器, 2012, 34(3): 79-82.

[20] Zhou X H, Wang Z Y, Wang L, et al. Propagation properties of high power ultrashort pulse in the gain medium[J]. Acta Photonica Sinica, 2010, 39(8): 1528-1532.
周小红, 王泽勇, 王黎, 等. 高功率超短脉冲在增益介质中的传输特性[J]. 光子学报, 2010, 39(8): 1528-1532.

Femtosecond Chirped Pulse Amplification System with Liquid Crystal Spatial Light Modulator for Spectral Modulation

Duan Yufei[1,2], Li Feng[1*], Yang Zhi[1], Li Qianglong[1], Yang Yang[1], Wu Tianhao[1,2], Wang Yishan[1], Yang Xiaojun[1**]

[1] *State Key Laboratory of Transient Optics and Photonics, Xi'an Institute of Optics and Precision Mechanics, Chinese Academy of Sciences, Xi'an, Shaanxi* 710119, *China;*

[2] *University of Chinese Academy of Sciences, Beijing* 100049, *China*

Abstract

Objective Compared with traditional solid-state lasers, such as slats and wafers, femtosecond fiber lasers have many advantages, including compact structures, good beam quality, stable systems, and good heat dissipation. They are widely used in various application fields, particularly in the field of fine material processing. The current femtosecond fiber laser is mainly used to reduce the problems of nonlinearity and device damage in the amplification process using the chirped pulse amplification technology to obtain a femtosecond laser with its peak power and narrow pulse width meeting processing requirements. Owing to the increase in the energy demand of an industrial fiber laser, the amplification classes also gradually increase, rendering the narrowing effect due to an uneven gain medium increasingly severe and influencing the final spectral width. Thus, its occurrence increases the compressed pulse width limit, reduces the pulse peak power, and severely impacts the thermal diffusion in processing. Currently, the gain narrowing problem of a femtosecond fiber laser can be solved using self-phase modulation, a new amplifying stage system, or dielectric layer filters. However, these approaches can only form fixed spectral modulation, which cannot solve the gain narrowing problem in different amplification or laser systems with different power requirements of the same amplification system. Therefore, programmable devices are proposed to achieve the controllability of spectral modulation. Among them, the liquid crystal spatial light modulator, a common element for beam shaping and pulse shaping, exhibits higher regulating precision than the general acousto-optic filter. For a fiber laser seed source, its spectral width is only a few nanometers or tens of nanometers; the liquid crystal spatial light modulator is more suitable for fiber laser spectral modulation. This study focuses on the characteristics of the spatial light modulator and the requirement of a chirp pulse amplification system for spectral modulation. The solutions of a spectral shaping system are proposed based on the two-dimensional (2D) intensity-type liquid crystal spatial light modulator for spectral modulation. The chirped pulse amplification system eliminates the gain narrowing problem and achieves a narrower output pulse duration.

Methods Herein, the 2D intensity-type liquid crystal spatial light modulator was used for spectral modulation. First, the seed source is amplified using the single-mode amplification system and enters the spectral shaping system, which comprises the polarization-splitting prism, grating, and the intensity of reflection-type liquid crystal spatial light modulator to perform various spectral modulation shapes and verify the programmability and high precision of the spectral shaping system. Then, the subsequent multi-mode amplification and main amplification systems with an optical fiber aperture of 25 μm were established. The shape required for spectral shaping, which can be compared with the initial spectrum function to achieve a 2D grayscale map, was obtained using the step-by-step Fourier transform method combined with reverse operation. Next, the grayscale image was loaded into the spatial light modulator, and the spectral widths before and after the addition of the grayscale image were compared to investigate the influence of the shaping system on the spectra and the reasons for the spectral shape formation. Finally, the near-limited output pulse duration of the femtosecond laser was obtained by compressing an appropriate distance by the 1450 line/mm grating, and the pulse duration was measured using an autocorrelation instrument to determine the optimization results of pulse duration.

Results and Discussions The spectrum can be reshaped into flat-top, central-depression, triangle, continuous-depression, and other shapes using the spectral shaping system (Fig. 4). Generally, as the spectral shaping becomes more complex and its shaping effect becomes worse, the modulation of the liquid crystal void generated using the liquid crystal spatial light modulator becomes increasingly obvious. After adding the main amplification system, the spectral width before entering the amplification system is reduced by approximately 1.5 nm (Fig. 5) and the gain

narrowing effect is evident. The grayscale map obtained using reverse operation was loaded on the 2D liquid crystal spatial light modulator to obtain the super-Gaussian spectral shape (Fig. 6) after spectral shaping and amplification. The full width at half maximum of this spectrum is approximately 9.5 nm. The spectral width is approximately 2.5 nm, and the corresponding limited pulse duration is reduced from 222 fs to approximately 164 fs. Finally, the pulse duration of 170 fs, close to the limit, can be obtained after the laser with spectral shaping is compressed through the grating. Compared with that of direct compression, the pulse duration is decreased by 86 fs. Moreover, the pulse shape has a side lobe owing to the liquid crystal spacing problem of the liquid crystal spatial light modulator (Fig. 7).

Conclusions Results show that the spectral shaping system can realize the arbitrary spectral modulation using the liquid crystal spatial light modulator. It can also set the spectral bandpass characteristics by regulating the function of different spectral component gains and realize dynamic matching using the subsequent amplification spectrum. Thus, this system is suitable for different conditions of gain spectrum modulation demand and can achieve a pulse duration close to the limit to meet the narrow output pulse duration and peak power of a femtosecond laser. Moreover, it achieves the purpose of efficient material cold working and satisfies the high requirements of the thermal effect for femtosecond laser applications. However, the improved results can be obtained using a modulator with a higher filling rate and smaller clearance for spectral shaping.

Key words lasers; spectral modulation; gain narrowing; chirped pulse amplification system; liquid crystal spatial light modulator; fiber femtosecond laser

OCIS codes 140.3510; 300.6360; 320.1590; 320.7090